Theoretical calculation of thermodynamic data for bcc binary alloys with the embedded-atom method

Zhang Bangwei
Chinese Center of Advanced Science and Technology (World Laboratory), P.O. Box 8730, Beijing 100080, People's Republic of China and Department of Physics, Hunan University, Changsha 410082, People's Republic of China

Ouyang Yifang
Department of Physics, Hunan University, Changsha 410082, People's Republic of China
(Received 9 June 1992; revised manuscript received 1 December 1992)

The dilute-limit heats of solution for all binary alloys of six bcc transition metals (V, Nb, Ta, Mo, W, and Fe) have been calculated with the analytic embedded-atom model for bcc pure metals by Johnson and Oh. Cubic equations are proposed and used for providing a smooth cutoff for the calculated potential and electron density functions between second- and third-nearest neighbors in the calculation. The heats of formation for all of the binary alloys of these six bcc metals for the whole compositional range and the intermetallic compounds A_3B, AB, and AB_3 are also calculated. The dilute-limit heats of solution are generally in agreement with available experimental values except for Ta in W and W in Ta. The heats of formation agree well with available experimental data, *ab initio* calculations by Colinet, Beesound, and Pasturrel, and thermodynamic calculations with the Miedema model for Mo-Ta, Mo-Nb, and Fe-V. The heats of formation are in good agreement with thermodynamic calculations with the Miedema model for W-V, Nb-V, Ta-V, Fe-W, Mo-W, Ta-Nb, Fe-Nb, Fe-Ta, and Mo-V alloy systems. There are, however, significant differences between the heats of formation for the present work and calculations with the Miedema model for the Ta-W, Nb-W, and Fe-Mo alloy systems.

I. INTRODUCTION

There is a lot of interest in modeling the heats of solution and formation ΔH for metallic alloys because of its importance. Miedema and co-workers[1,2] calculated the heats of solution and formation for a number of alloy systems by an empirical model from thermodynamics. The theoretical results are generally in good agreement with available experimental data. The agreement between them, however, still needs improvement because assumptions and approximations are made in the model and calculations. First-principles calculations for heats of formation should be attractive methods because of their microscopic physics premise. Several calculations with the *ab initio* calculations have been performed. For example, Terakura and co-workers[3–5] performed local-density-functional band calculations of ΔH for alloys which are composed of Cu, Ag or Au as one element and one of Ni, Pd or Pt as the other element. Colinet, Beesound, and Pasturral[6] performed calculations of ΔH for Cr-W, Cr-Mo, Mo-W, Mo-Ta, Mo-Nb, and Ta-W alloys based on an alloy cluster-Bethe-lattice method. All of the results are in good agreement with available experimental values. However, the *ab initio* methods are generally limited to very small systems, and various degrees of approximation should be involved in the methods when solving Schrödinger's equation. It is therefore not easy to apply them to all kinds of alloy systems.

The embedded-atom method (EAM) developed by Daw and Baskes[7] is a powerful tool to describe the problems for metals and alloys. Johnson[8–10] has developed an analytic nearest-neighbor embedded-atom model for fcc metals and alloys, and calculated the dilute-limit heats of solution for all fcc binary alloys of Cu, Ag, Au, Ni, Pd, and Pt, and the heats of formation for 12 binary alloys of these fcc metals. The results are generally in good agreement with the available experimental data and *ab initio* calculations by Terakura and co-workers, but their model fails to predict Pd alloys, which indicate that the model is effective for calculating ΔH of fcc alloys at least. Johnson and Oh[11] have developed an analytic nearest-neighbor embedded-atom-method model for bcc metals. Guellil and Adams have performed a brief study of alloy heats of solution of bcc alloys for Fe in V, V in Fc, K in Na, and Na in K, with the EAM of Johnson and Oh.[12] In addition this scheme cannot generate a model for Cr because the elastic constants of Cr require a negative curvature of the embedding function. In this paper, the dilute-limit heats of solution and heats of formation for 15 binary alloys of all bcc transition metals, (V, Nb, Ta, Mo, W, and Fe) except Cr were calculated using the analytic nearest-neighbor bcc model and its extension to alloys according to the same procedures by Johnson from fcc metals to fcc alloys. A cubic equation has been proposed for the cutoff potential for a two-body potential.

This paper is organized as follows. The model and the procedures used in the paper are described in Sec. II. The calculation results and discussions will be presented in Sec. III, and the conclusions are made in Sec. IV.

II. THEORETICAL MODEL

The basic equations of the embedded-atom-method model are

$$E_t=\tfrac{1}{2}\sum_{ij}{}'(r_{ij})+\sum_i F(\rho_i)\ , \tag{1}$$

$$\rho_i=\sum_j{}' f(r_{ij})\ , \tag{2}$$

where E_t is the total internal energy, ρ_i is the electron density at atom i due to all other atoms, $f(r_{ij})$ is the electron density at atom i due to atom j as a function of the distance between them, r_{ij} is the separation distance between atoms i and j, $F(\rho_i)$ is the energy to embed atom i in an electron density ρ_i, and $\phi(r_{i,j})$ is a two-body potential between atoms i and j.

In order to apply the model, the embedding function $F(\rho)$, atomic electron-density function $f(r)$, and the two-body potential function must be known. Because the electron density at any location is approximated by the linear superposition of atomic electron densities, the same function of it in the pure metal can be used for an alloy. Therefore, we have[11]

$$f(r)=f_e(r_{1e}/r)^{\beta}\ . \tag{3}$$

f_e is the scaling factor, which is determined by the relation of $\rho_e=E_c/\Omega$. From Eq. (2), it is given by

$$f_e=E_c/(S_\beta\Omega) \tag{4}$$

$$S_\beta=\sum_{i=1}^{n} N_i/k_i^{\beta}\ , \tag{5}$$

where the sum is over neighbor shells, N_i is the number of atoms in the ith shell, and k_i is the ratio of the radius of the ith shell to the nearest-neighbor distance, $r_i=k_i r_1$. $S_\beta=8+3\sqrt{3}$ when the first- and second-nearest-neighbor shells are only taken into account. E_c is the cohesive energy, Ω is the atomic volume, r_{1e} is the equilibrium first-neighbor distance, and β is an adjustable parameter. $\beta=6$ is used for all of the alloys. It will be seen below that only ratios of electronic densities occur in the representations of $F(\rho)$ and alloy potentials $\phi^{ab}(r)$; the scaling contant S_β cancels from the model, so it is taken as 1 for convenience. Because the embedding energy in the EAM model is assumed to be independent of the source of the electron density, the embedding function can be also taken directly from monatomic model, which is

$$F(\rho)=-(E_c-E_{1f})[1-\ln(\rho/\rho_e)^n](\rho/\rho_e)^n\ . \tag{6}$$

Here E_{1f} is the unrelaxed vacancy formation energy, ρ_e is the equilibrium electron density, and n is a parameter that is given by

$$n=\frac{1}{\beta}\left[\frac{9\Omega B-15\Omega G}{E_c-E_{1f}}\right]^{1/2}\ , \tag{7}$$

where B is the bulk modulus, and G is the Voigt average shear modulus.

The two-body potential function in an alloy could be determined from the monatomic potentials when sufficient data were available. However, it is usually determined from the assumption that the alloy potential is a function of the monatomic potentials. The same type of function as in fcc alloys,[9]

$$\phi^{ab}(r)=\frac{1}{2}\left[\frac{f^b(r)}{f^a(r)}\phi^{aa}(r)+\frac{f^a(r)}{f^b(r)}\phi^{bb}(r)\right]\ , \tag{8}$$

is used for all alloy potentials of bcc alloys. The superscripts a and b indicate the a- and b-type atoms in a binary alloy. $\phi^{aa}(r)$ and $\phi^{bb}(r)$ are the monatomic potentials which could be given by the monatomic models. This alloy potential is in a normalized form, i.e., the effective two-body potential, for which a term linear in the electron density is added to or subtracted from the embedding function and an appropriate adjustment is made to the two-body potential. The monatomic potential is taken as a spline function[11]

$$\phi(r)=k_3\left[\frac{r}{r_{1e}}-1\right]^3+k_2\left[\frac{r}{r_{1e}}-1\right]^2+k_1\left[\frac{r}{r_{1e}}-1\right]+k_0\ . \tag{9}$$

The parameters k_3, k_2, k_1, and k_0 are as follows:

$$k_3=-\frac{15\Omega G}{3A+2}\left[\frac{3}{4}A-\frac{1}{2}S\right]\ , \tag{10}$$

$$k_2=-\frac{15\Omega G}{3A+2}\left[\frac{15}{16}A-\frac{3}{4}S-\frac{9}{8}AS+\frac{7}{8}\right]\ , \tag{11}$$

$$k_1=-15\Omega G\left[\frac{7}{8}-\frac{3}{4}S\right]\ , \tag{12}$$

$$k_0=-\frac{15\Omega G}{3A+2}\left[\frac{201}{112}A-\frac{27}{28}S-\frac{87}{56}AS+\frac{187}{168}\right]-\frac{1}{7}E_{1f}\ , \tag{13}$$

where $A=C/C'$ is the anisotropy ratio, with $C=C_{44}$, $C'=1/2(C_{11}-C_{12})$, and $S=r_{2e}/r_{1e}=2/\sqrt{3}$.

It was found that the monatomic potential is rather soft at short interatomic distances,[11] so to stiffen it, the modification

$$\phi_a(r)=\phi(r)+k_a[\phi(r)-\phi(r_{1e})](r/r_{1e}-1)^2 \tag{14}$$

is used for $r<r_{1e}$ with the parameter k_a taken as

$$k_a=4.5[1+4/(A-0.1)]\ . \tag{15}$$

For providing a smooth cutoff for both $\phi(r)$ and $f(r)$, an appropriate cutoff potential and cutoff electron-density function between second- and third-nearest neighbors must be specified. A similar cubic spline function is used for the cutoff potential $\phi_b(r)$ between second- and third-neighbor distances. The cutoff electron-density function $f_b(r)$ is also a cubic spline function. The cutoff procedure is such that the cutoff potential and electron density have smoothly matching values and slopes to the calculated potential and electron density, respectively, at second-neighbor distance r_{2e}, and have zero value and slope at the point of three-fourths of second- to third-nearest neighbors, i.e., $r_c=r_{2e}+3/4(r_{3e}-r_{2e})$. For potential, therefore, we have

$$\phi(r_{2e})=\phi_b(r_{2e}) , \tag{16}$$

$$\phi'(r_{2e})=\phi_b'(r_{2e}) , \tag{17}$$

$$\phi_b(r_c)=0 , \tag{18}$$

$$\phi_b'(r_c)=0 , \tag{19}$$

where $\phi_b(r)$ is the cutoff potential. For electron density we also have similar equations from (16)–(19). The cutoff potential then is taken as

$$\phi_b(r)=1_3(r/r_{2e}-1)^3+1_2(r/r_{2e}-1)^2+1_1(r/r_{2e}-1)+1_0 , \tag{20}$$

with

$$1_3=\frac{1}{(\gamma-1)^3}[21_0+(\gamma-1)l_1]$$
$$=-\frac{15\Omega G}{(3A+2)(\gamma-1)^3}\left[\left[\frac{8}{7}+3\gamma\right]AS-\left[\frac{9}{7}+\frac{7}{2}\gamma\right]A+\left[\frac{4}{7}+2\gamma\right]S-\left[\frac{40}{63}+\frac{7}{3}\gamma\right]\right]-\frac{2}{7(\gamma-1)^3}E_{1f} , \tag{21}$$

$$1_2=\frac{1}{(\gamma-1)^2}[-31_0-2(\gamma-1)l_1]$$
$$=\frac{15\Omega G}{(3A+2)(\gamma-1)^2}\left[\left[\frac{3}{14}+6\gamma\right]AS-\left[\frac{5}{28}+7\gamma\right]A-\left[\frac{1}{7}-4\gamma\right]S-\left[\frac{3}{14}+\frac{14}{3}\gamma\right]\right]+\frac{3}{7(\gamma-1)^2}E_{1f} , \tag{22}$$

$$l_1=-\frac{15\Omega G}{3A+2}\left[3AS-\frac{7}{2}A+2S-\frac{7}{3}\right] , \tag{23}$$

$$l_0=-\frac{15\Omega G}{3A+2}\left[\frac{29}{14}AS-\frac{67}{28}A+\frac{9}{7}S-\frac{187}{126}\right]-\frac{1}{7}E_{1f} , \tag{24}$$

where $\gamma=r_c/r_{2e}$. The cutoff electron density is taken as

$$f_b(r)=m_3(r/r_{2e}-1)^3+m_2(r/r_{2e}-1)^2+m_1(r/r_{2e}-1)+m_0 , \tag{25}$$

with

$$m_3=f_eS^{-\beta}[2-\beta(\gamma-1)]/(\gamma-1)^3 , \tag{26}$$

$$m_2=-f_eS^{-\beta}[3-2\beta(\gamma-1)]/(\gamma-1)^2 , \tag{27}$$

$$m_1=-\beta f_eS^{-\beta} , \tag{28}$$

$$m_0=f_eS^{-\beta} . \tag{29}$$

The dilute-limit heats of solution of binary alloys for solute b in solvent a are the summation of the four following terms.

(a) The energy results from removing a host atom:

$$E_1=-F^a(\rho_e^a)-8\phi^{aa}(r_{1e}^a)-6\phi^{aa}(r_{2e}^a) . \tag{30}$$

(b) The energy results from adding an impurity atom:

$$E_2=F^b(\rho_e^a)+8\phi^{ab}(r_{1e}^a)+6\phi^{ab}(r_{2e}^a) . \tag{31}$$

(c) The energy results from the effects on the neighbor atoms caused by adding an impurity atom:

$$E_3=-14F^a(\rho_e^a)+8F^a(\rho_e^a+\Delta\rho)+6F^a(\rho_e^a+\Delta\rho') , \tag{32}$$

where

$$\Delta\rho=-f^a(r_{1e}^a)+f^b(r_{1e}^a) , \tag{33}$$

$$\Delta\rho'=-f^a(r_{2e}^a)+f^b(r_{2e}^a) . \tag{34}$$

(d) The energy results from the change of cohesive energy after the host atom was replaced by the impurity atom:

$$E_4=-E_c^a+E_c^b . \tag{35}$$

Therefore,

$$E=E_1+E_2+E_3+E_4 . \tag{36}$$

The heats of solution calculated above are unrelaxed values. The relaxation energy for elastic distortion of lattice caused by the difference of sizes between the host and impurity atoms must be considered. According to Friedel,[13] the relaxation energy can be approximated by the relation

$$E=\frac{24\pi BGr_0r_1(r_1-r_0)^2}{3Br_1+4Gr_0} , \tag{37}$$

where r_0, r_1 are the atomic radii for the pure elements of host and impurity, respectively, B is the bulk modulus of the impurity, and G is the shear modulus of the host.

The heats of formation for the disordered alloys with any composition and the ordered intermetallic compounds A_3B, AB, and AB_3 are the differences of energies substracting the cohesive energies for the pure constituents from the total energies for the binary alloys with specified structures. In the calculations for the heats of formation, the structures of the alloys, whether disordered or ordered, were assumed to have a bcc lattice. For the disordered alloys with any composition, the probability occupying the lattice sites for a constituent of an

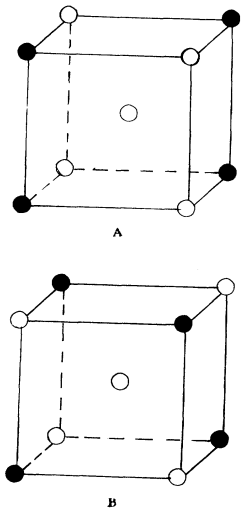

FIG. 1. Two possible bcc structures for an A_3B ordered alloy: ○, A atom; ●, B atom.

alloy is the atomic percent of the constituent in the alloy. For the ordered AB-type compounds, there is only one possible structure, i.e., A occupies the center sites and B the angular sites of the bcc lattice. The occupied probabilities for A and B are the same. As for A_3B or AB_3 compounds, there are two possible ordered structures, as shown in Fig. 1. The calculations of the heats of structure of Fig. 1(b) is more stable than that of (a) because the heats of formation for (b) are less than that for (a). For example, it is -0.087 eV/atom for (b), and -0.081 eV/atom for (a) for the compound Nb_3Mo. The structure of Fig. 1(b) was therefore used in the calculation.

III. RESULTS AND DISCUSSIONS

The input physical quantities a, E_c, ΩB, ΩG, A, and E_{1f} are all taken from experimental data, which are shown in Table I. The lattice and elastic constants are room-temperature data, while the cohesive energy is for absolute zero.

The model parameters k_3, k_2, k_1, k_0, l_3, l_2, l_1, l_0, m_3, m_2, m_1, m_0, k_a, f_e, and n calculated from the input physical quantities are shown in Table II.

A. Dilute-limit heats of solution

Table III lists the dilute-limit heats of solution for all binary alloys of the six bcc metals V, Nb, Ta, Mo, W, and Fe. Shown in the first row are the values of the unrelaxed calculations, the second row shows the values with the approximation for relaxation, and the available experimental data are shown in the third. The comparisons for the heats of solution between the calculated values with and without relaxation and experimental data are illustrated in Fig. 2. It can be seen from Fig. 2 that the agreement between the calculated values with relaxation and experimental data is very good except for those of Ta in W and W in Ta. That comparison indicates an overall improvement for the alloys of Mo in Nb, Fe in V, Ta in W, and W in Ta, but indicates a change for the worse for the alloys of Nb in Mo and V in Fe after the calculation with relaxation was performed. But this is only a preliminary conclusion because of limited available experimental data.

Since the values of input parameters are not definite exact quantities, but in a range, e.g., the vacancy formation energy for W is from 3.3 to 4.0 eV,[19] the calculated heats of solution, therefore, are dependent on the selection of values for input parameters. The calculated heats for W in Ta and Ta in W with and without relaxation are all positive, which are all contrary to the experimental data, and which indicates that the scheme is still in need of improvement in spite of how to select the value for the vacancy formation energy in the range. 3.3 eV for the vacancy formation energy of W was used in this paper.

B. Heats of formation

The calculated heats of formation for 15 binary alloys of six bcc metals are shown in Fig. 3. The dot and solid line shows the results for the disordered alloys with any composition, and Δ represents the results for the ordered intermetallic compounds A_3B, AB, and AB_3. For comparison, the available experimental data (+), the *ab initio* calculations by Colinet, Beesound, and Pasturral,[6] (▲), and the results of the thermodynamic calculations of Miedema and co-workers,[1,2] (■) are also indicated in Fig. 3.

The results of Mo-Ta and Mo-Nb systems are in excellent agreement with the available experimental data and the calculations of Colinet, Beesound, and Pasturral and Miedema and co-workers, respectively. The phase diagrams for the alloy systems are all series solid solutions,

TABLE I. Input physical quantities for six bcc metals. a in Å, E_c, ΩB, ΩG, and E_{1f} are all in eV. A is dimensionless. The input quantities are the same as that used by Johnson and Oh (Ref. 11) except for E_{1f}.

Metal	a (Ref. 14)	E_c (Ref. 15)	ΩB (Ref. 16)	ΩG (Ref. 16)	A (Ref. 16)	E_{1f}
V	3.0399	5.30	13.62	4.17	0.78	2.10 (Ref. 17)
Nb	3.3008	7.47	19.08	4.43	0.52	2.04 (Ref. 18)
Ta	3.3026	8.089	21.66	7.91	1.57	2.18 (Ref. 19)
Mo	3.150	6.810	25.68	12.28	0.78	3.22 (Ref. 19)
W	3.164 75	8.66	30.65	15.84	1.01	3.30 (Ref. 20)
Fe	2.866 45	4.29	12.26	6.53	2.48	1.79 (Ref. 21)

TABLE II. Model parameters for six bcc metals, k_i, l_i, and m_i ($i=0,1,2,3$) in eV, f_e in eV/Å^3, and k_a and n are dimensionless.

Metal	k_3	k_2	k_1	k_0	l_3	l_2	l_1	l_0	m_3	m_2	m_1	m_0	k_a	f_e	n
V	−0.11	3.94	−0.56	−0.30	−11.99	4.38	0.75	−0.30	0.72	1.20	−0.96	0.16	30.97	0.38	0.72
Nb	3.50	3.34	−0.60	−0.29	−11.18	3.93	0.80	−0.29	0.80	1.32	−1.05	0.18	47.36	0.42	0.73
Ta	−10.61	9.88	−1.07	−0.33	−4.83	−0.04	1.42	−0.29	0.86	1.43	−1.14	0.19	16.75	0.45	0.60
Mo	−0.33	11.59	−1.65	−0.47	−7.07	−0.25	2.20	−0.45	0.83	1.39	−1.10	0.18	30.97	0.44	0.60
W	−8.51	16.83	−2.13	−0.49	−0.42	−4.38	2.84	−0.45	1.05	1.74	−1.38	0.23	24.28	0.55	0.45
Fe	−13.31	9.21	−0.88	−0.27	−3.57	−0.22	1.17	−0.24	0.70	1.16	−0.92	0.15	12.06	0.36	0.37

and the crystal structures of alloys in whole composition range are bcc, which indicates our assumption is consistent with the facts. Also, the relative differences $\Delta a/a$ of the lattice constants for the elements of the alloys are all less than 5%; the elastic energies resulting from the effects, therefore, are not the primary influence in alloying. This excellent agreement therefore should be easily understood. The results of Fe-V alloys are all negative and are in good agreement with the available experimental data. Although our calculated values are larger than the data, the values calculated by Miedema and co-workers are less than the data. For Fe-V system, although the value of $\Delta a/a$ is only 6%, but there is a little complexity in its phase diagram because the σ phase occurs in a certain composition range at rather low temperatures, which implies the structures of the alloys in the range are not bcc. Also, the calculations were performed at room temperature, while the experimental data given were at 1065 K.[22] We consider these facts as reasons for the difference between the calculated values and the data. The present calculations give negative values for the Mo-W system, while the Colinet values are positive, though the negative values are rather small, and the positive values are almost close to zero. Which value is in agreement with experimental data cannot be known because no such data is available at this time.

The problem is in the system of Ta-W. The calculated values are positive though they are very small and close to zero. But the experimental data and the values calculated by Colinet, Beesound, and Pasturral and by Miedema and co-workers are all negative. The phase diagram for the system is a series solid solution, and the $\Delta a/a$ is only 4%. These factors are favored to reduce the difference between the calculations and experimental data. The fact that the calculations and experimental data were carried out at different temperatures cannot be solely responsible for this difference of the heats of formation. The most probable explanation is that the present model may not be a reliable method for the calculations of the Ta-W system.

There are also no experimental data or *ab initio* calculations for the V-Ta, V-W, V-Mo, V-Nb, Nb-W, and Nb-Ta systems. The phase diagrams for these systems are all series solid solutions, and the $\Delta a/a$ are all less than 4% except less than 9% for V-Nb and V-Ta systems, which means that these factors do not result in considerable effects on the calculations of their heats of formation. The present results are generally in agreement with the calculations by Miedema and co-workers. There is a rather large difference for V-Mo alloys, in which the present calculations are positive, while the values of Miedema and co-workers are almost zero.

The present results for Fe-Nb, Fe-Ta, and Fe-W alloys are comparable to those of calculations by Miedema and

TABLE III. Dilute-limit heats of solution for all binary alloys of the six bcc metals V, Nb, Ta, Mo, and W, and Fe. The first row is the values of the unrelaxed calculations, the second row is the values with the approximation for the relaxation, and the third is the experimental data available. All energies are in eV.

Host	V	Nb	Ta	Mo	W	Fe
V		−0.49	−0.62	0.14	−0.05	−0.09
		−0.57	−0.74	0.11	−0.09	−0.15
						−0.16 (Refs. 2 and 22)
Nb	−0.57		0	−0.35	0.22	−1.29
	−0.66		0	−0.41	0.17	−1.67
				−0.27 (Ref. 23)		
Ta	−0.61	0.01		−0.49	0.08	−1.29
	−0.71	0.01		−0.55	0.02	−1.69
					−0.22 (Ref. 24)	
Mo	0.17	−0.31	−0.48		−0.15	0.22
	0.15	−0.34	−0.53		−0.15	0.03
		−0.42 (Ref. 23)				
W	−0.04	0.16	0.04	−0.16		−0.35
	−0.06	0.13	0	−0.16		−0.56
			−0.31 (Ref. 24)			
Fe	0	−0.23	−0.38	0.31	−0.18	
	−0.04	−0.46	−0.72	0.12	−0.42	
	−0.10 (Ref. 25)					

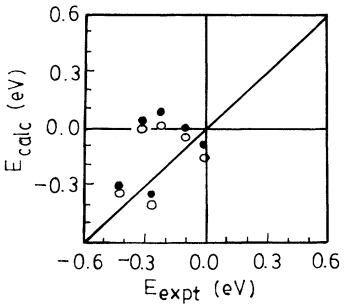

FIG. 2. The calculated dilute-limit heats of solution with (○) and without (●) relaxation vs the available experimental data for bcc binary alloys.

co-workers. But the heats of formation for Fe-Mo alloys are just contrary: The present calculations are positive, while the values of Miedema and co-workers are negative. Considering the experimental values[2] for the four alloys (Fe=44, 60, 61, and 67 at %), the present results come closer to the data than the values of Miedema and co-workers. That is, however, a somewhat surprising result because the phase diagrams for the four-alloy systems are all complex, and our assumption is that they all have bcc structures.

From the calculated values for A_3B, AB, and AB_3 intermetallic compounds with bcc structure, it can be seen that they are generally in agreement with the available experimental data. It is also interesting to note that some of the calculations for the ordered phases are far below those of the disordered phases. It is well known that there is a positive entropy stemming from the disordered arrangement of atoms in a disordered alloy, but no such entropy exists in an ordered alloy. The positive entropy would reduce the calculated enthalpy in an alloy. In fact, the measured entropies are all positive for some alloys in Nb-Mo, Mo-Ta, Ta-W, Fe-V, Fe-Mo, Fe-W, and Fe-Ta systems, e.g., $+4.9\times10^{-5}$ eV/K for the $Mo_{50}Ta_{50}$ alloy measured at 1200 K.[2] de Boer *et al.*[2] have also pointed this out when they discussed the fact that their predictions for ordered compounds are more negative than the predictions by Colinet, Pasturrel, and Hicter[27] for disordered alloys. The present calculated results, therefore, are reasonable and believable.

From all the above-mentioned facts and discussions we may conclude that the present scheme is generally effective for calculations of heats of formation for bcc metal alloys except for the Ta-W system.

From the present calculations it can be seen that the heats of formation are all small if the relative differences

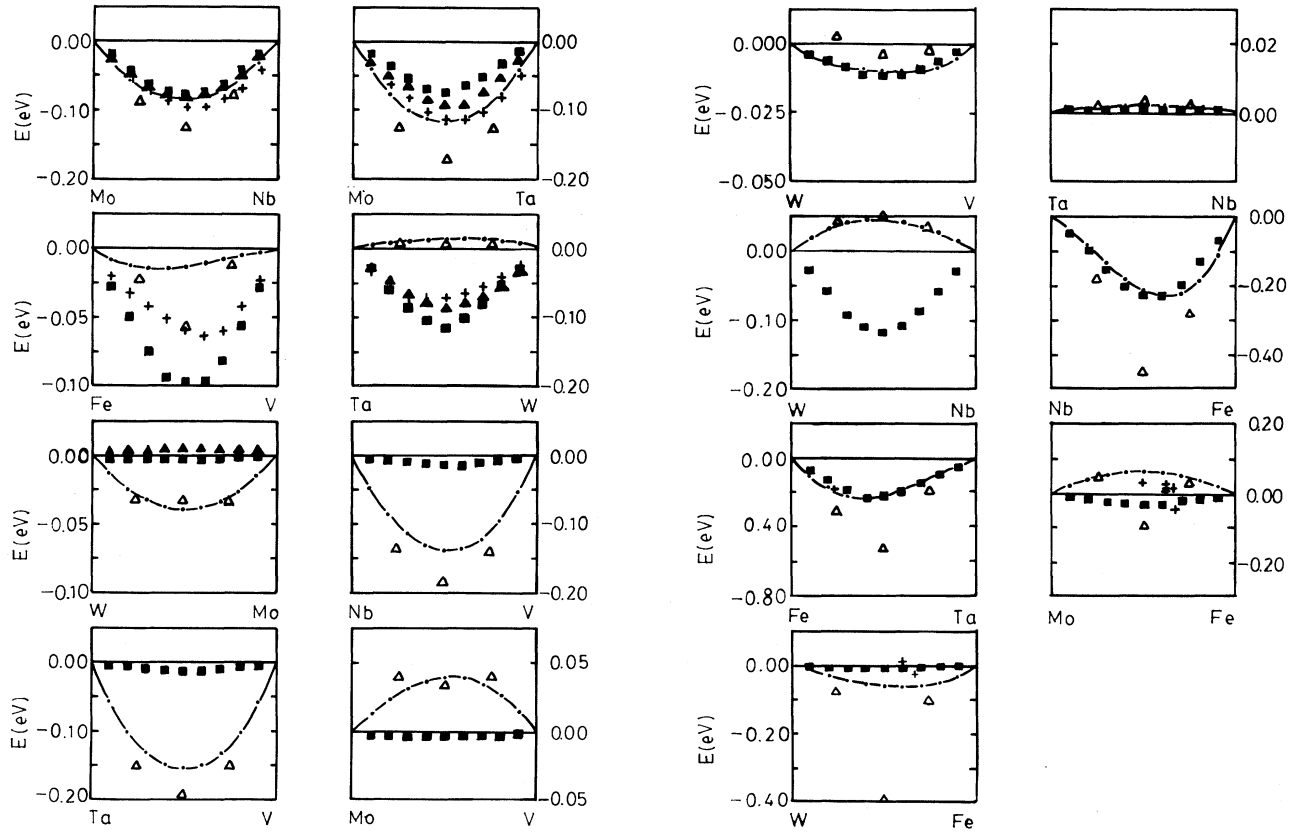

FIG. 3. Heats of formation vs compositions for 15 binary alloys of V, Nb, Ta, Mo, W, and Fe metals. The dots and solid lines are the present calculated results for disordered alloys. △ shows the present results for ordered intermetallic compounds A_3B, AB, and AB_3. + indicates the experimental data. ▲ and ■ are the calculated results by Colinet, Beesound, and Pasturrel and Miedema and co-workers, respectively. The experimental data are from Ref. 26 for the Mo-Ta system, Ref. 22 for Mo-Nb, Ref. 24 for Ta-W, Ref. 22 for Fe-V, and Ref. 2 for the Fe-Nb, Fe-Ta, Fe-Mo, and Fe-W systems, respectively.

of the sizes and cohesive energies between the two elements are small, e.g., in Nb-Ta, Mo-W, and V-Mo systems the two quantities are not larger than 4 and 29 %, respectively, and the heats of formation for them are indeed small. Otherwise the heats of formation, e.g., for the Fe-W, Fe-Nb, Fe-Mo, and Fe-Ta systems, are large because the two quantities for these systems are large, which are from 9 to 15 % and 40 to 100 %, respectively. The primary factors controlling alloy heats of formation are the relative size and cohesive energy of the two metals, which is the same conclusion found in fcc metal alloys.[9,10] However, the conclusion that the heats of formation for fcc metals are negative if these two quantities are smaller for one metal than the other, and are positive if one is smaller and the other larger,[9,10] is not obtained in the present case. For example, the two quantities for one metal are both larger than those for another metal for the Mo-Fe and Ta-Fe systems, but the heats of formation for Mo-Fe are positive and negative for Ta-Fe, which is no simple explanation.

Our calculations show that the results would be bad if no cutoff procedure was used in the present scheme because the supposing potential and electron density were not the exact ones. The results were also dependent on what cutoff procedure was used. Two points should be noted for the cutoff procedure. One is about the selection for the starting point r_s. As pointed out in Ref. 11, r_s should be $\geq r_{2e}$. But where is the best point? The calculations show that $r_s = r_{2e}$ is the best point, and the results indicate a change for the worse if $r_s > r_{2e}$ when the end point r_c is not changed. Another is about the definition for r_c. The results show that the agreement between the calculations of heats and the available experimental data is improved with increasing the cutoff distance between second- and third-nearest neighbors, but the improvement will be very small when $r_c > r_{2e} + 3/4(r_{3e} - r_{2e})$. That is why $r_c = r_{2e} + 3/4(r_{3e} - r_{2e})$ is taken in the scheme.

This scheme cannot be used to calculate the heats of formation for the alloys containing Cr because $9\Omega B - 15\Omega G$ of Cr is negative, which leads to the parameter n and the embedding function has no meaning. To complete such calculations another EAM scheme should be presented.

IV. CONCLUSIONS

To calculate the heats of formation for bcc metal alloys some revisions, mainly about the cutoff potential $\phi_b(r)$ and cutoff electron density $f_b(r)$ and the cutoff distance, are made for the analytic embedded-atom model for bcc pure metals by Johnson and Oh. Using the scheme the dilute-limit heats of solution and the heats of formation for all binary alloys of six bcc transition metals, V, Nb, Ta, Mo, W, and Fe are calculated with no adjustable parameters.

The calculated dilute-limit heats of solution are in good agreement with the available experimental data after the calculations were improved with relaxation. But the calculated heats of solution for Ta in W and W in Ta alloys are positive, while the experimental data are negative.

The calculated heats of formation for the 15 binary disordered alloys of six bcc metals with any composition are generally in agreement with the available experimental data, the *ab initio* calculations, and the thermodynamic calculations except for the Ta-W, Nb-W, and Fe-Mo systems, for which the present values are positive, while the thermodynamic calculations are negative.

The calculated heats of formation for the ordered intermetallic compounds A_3B, AB, and AB_3 of the alloy systems have the same sign of the heats of formation for the disordered alloys in the same alloy system. But the former are generally less than the later. The only exception occurs also in the Fe-Mo system, for which the heat of formation for the FeMo compound is negative.

The heats of formation are small if the relative differences of the sizes and cohesive energies between two metals are both small, otherwise, they are large if the two quantities are both large.

ACKNOWLEDGMENTS

It is a pleasure to acknowledge stimulating and helpful discussions with Professor R. A. Johnson at the University of Virginia. This work was supported by the National Natural Science Foundation.

[1] A. R. Miedema, P. F. de Chatel, and F. R. de Boer, Physica **100B**, 1 (1980).
[2] F. R. de Boer, R. Boom, W. C. M. Mattens, A. R. Miedema, and A. K. Niessen, *Cohesive in Metals,* 2nd ed. (North-Holland, Amsterdam, 1989).
[3] K. Terakura, T. Oguchi, T. Mohri, and K. Watanabe, Phys. Rev. B **25**, 2169 (1987).
[4] K. Terakura, T. Mohri, and T. Oguchi, Mater. Sci. Forum **37**, 39 (1989).
[5] S. Takazawa and K. Terakura, Phys. Rev. B **39**, 5792 (1989).
[6] C. Colinet, A. Beesound, and A. Pasturrel, J. Phys. F. **18**, 903 (1988).
[7] M. S. Daw and M. I. Baskes, Phys. Rev. B **29**, 6443 (1984).
[8] R. A. Johnson, Phys. Rev. B **37**, 3924 (1988).
[9] R. A. Johnson, Phys. Rev. B **39**, 12 554 (1989).
[10] R. A. Johnson, Phys. Rev. B **41**, 9717 (1990).
[11] R. A. Johnson and D. J. Oh, J. Mater. Res. **4**, 1195 (1989).
[12] A. M. Guellil and J. B. Adams, J. Mater. Res. **7**, 639 (1992).
[13] J. Friedel, Adv. Phys. **3**, 446 (1954).
[14] *American Institute of Physics Handbook* (McGraw-Hill, New York, 1957).
[15] C. Kittel, *Introduction to Solid-State Physics,* 4th ed. (Wiley, New York, 1971), p. 96.
[16] G. Simmons and H. Wang, *Single Crystal Elastic Constants and Calculated Aggregate Properties: A Handbook,* 2nd ed. (MIT, Cambridge, MA, 1971).
[17] K. Slater, M. Reo, B. Saile, H. E. Schaefer, and A. Seeger, Philos. Mag. A **40**, 707 (1979).
[18] Seung-Am Cho, Z. Metallkd. **71**, 47 (1980).
[19] A. R. Miedema, Z. Metallkd. **79**, 345 (1979).
[20] H. Schultz, Acta Metall. **12**, 761 (1964).
[21] M. W. Finnis *et al.*, Philos. Mag. A **50**, 45 (1984).

[22]O. Kubschewski, H. Probst, and K. H. Geioer, Z. Phys. Chem. Neue Folge **104**, 23 (1977).
[23]S. C. Singhal and W. L. Worrell, Metall. Trans. **4**, 1125 (1973).
[24]S. C. Singhal and W. L. Worrell, Metall. Trans. **4**, 895 (1973).
[25]R. Hultgren, P. D. Desai, D. T. Hawkins, M. Gleiser, and K. K. Kelly, *Selected Values of the Thermodynamic Properties of Binary Alloys* (American Society for Metals, Metals Park, OH, 1973).
[26]S. C. Singhal and W. L. Worrell, in *Proceedings of the Symposium on Metallurgical Chemistry,* edited by D. Kubaschewski (Her Majesty's Stationary Office, London, 1972), p. 65.
[27]C. Colinet, A. Pasturrel, and P. Hicter, Physica **128B**, 5 (1985).